Nwosu Cajethan[1,*], Uchenna U. C.[2], Madueme Theophilus[1]

J. Electrical Systems 8-3 (2012): 304-316

Wind-Solar Hybrid Power System for Rural Applications in the South Eastern States of Nigeria

Journal of Electrical Systems

A combination of wind and solar resources offers a unique possibility in generating electricity either as grid-connected or as stand alone hybrid power system. This paper investigates the marrying of the two resources where one, solar, is in abundant and the other, wind, is in limited supply. A case study of Nsukka is presented with data obtained at the Centre for Basic Space Science, University of Nigeria, Nsukka. The model power plant simulates a combination of a variable speed wind turbine and 6 by 2 solar PV array with the aim to satisfy the load demand of a 3-bedroom flat apartment and to charge a battery bank during the period of excess power. The battery bank supplies the load in the event of hybrid power deficiency. The model at the end gives hope that the low wind resource can be hybridized with the high solar profile to generate firm power for stand alone or grid-connected systems.

Keywords: Hybrid system; low wind resource; solar insolation; load demand.

1. Introduction

An average wind speed of 5.8 m/s and above are considered good wind resource, while average wind speed below 4.5 m/s is considered a small wind resource [1]. Nigeria with average wind speed ranging between 2.5 m/s at the coastal areas to 4.5 m/s at the northern boundaries, therefore, falls within the low wind resource zone. But by no means does this natural placement constitute any threat to the application and utilization of wind energy in Nigeria's electric power system. But then what nature may deny Nigeria in wind resource it endows it abundantly in solar energy resource. The latitude and longitude of Nigeria is 10^o N and 8^o E, while for Nsukka they are approximately 7^o N and 7^o E. Going by Fig. 1, the trace of solar insolation for Nigeria and hence Nsukka should lie between the traces for latitudes 0^o N and 30^o N, but closer to that for latitude 0^o N. From Fig. 1 it can be inferred that large amount of solar radiation falls on Nigeria between January and December every year.

A combination of the two resources, wind and solar, therefore offers a unique possibility in generating electricity in Nigeria, either as grid-connected or as stand alone. Research studies have been carried out by several authors in the past to prove the unique possibility in combining renewable resources, wind and solar, in conjunction with backups to provide not just firm but green power [3], [4], [5], and [6]. These studies and many others focus on the regions where the wind speed variation may range from 5 m/s to 25 m/s with moderate sunshine. Published literature addressing the hybrid system in a region of small wind resource with high profile for sunshine is scanty [7], [8]. This paper, therefore, focuses on the applicability of wind-solar hybrid power system in a small wind and high sunshine region of South Eastern Nigeria, using Nsukka as a case study.

[*] Corresponding author: C. A. Nwosu, Department of Electrical Engineering, University of Nigeria, Nsukka, Nigeria, E-mail: cajethan.nwosu@unn.edu.ng
[1] Department of Electrical Engineering, University of Nigeria, Nsukka, Nigeria
[2] Department of Electrical/Electronic Engineering, Ambrose Alli University, Ekpoma, Nigeria

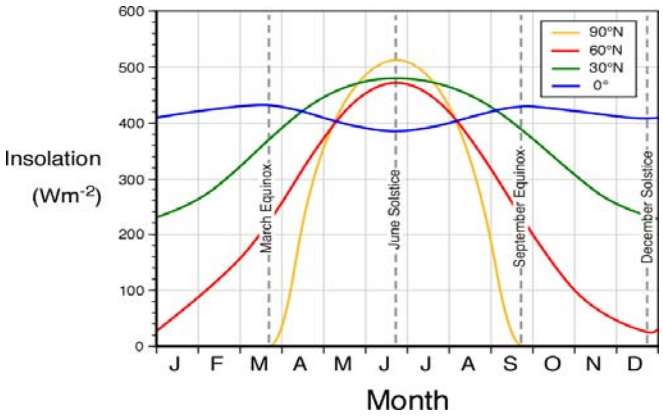

Fig. 1: Global traces of solar insolation between latitudes 0^o to 90^o [2].

2. System structure

The system structure proposed for the hybrid power plant is made up of two principal generators: the wind turbine generator and the PV generator (Fig. 2). It also has an energy storage that can act as a load or as a generator depending on the need. In order that maximum energy in the wind is utilized in this hybrid system, a variable speed wind turbine employing doubly-fed induction machine as its generator is used. Interposing the wind turbine and the generator is a gearbox, the function of which is to match the slow speed of the wind turbine with the high speed of the generator.

The PV generator comprises the PV unit and the inverter unit. The PV unit comprises parallel and series connected PV panels, while the inverter unit comprises a number of parallel connected inverters.

Under normal operation, the load is supplied by the interconnection of wind and solar power. Surplus energy from the hybrid system is stored in the battery. The battery component of the hybrid power plant is composed of two sets of battery banks BB1 and BB2. Power from BB1 is supplied to the autonomous bus through a current source inverter and thus presents itself for control. Power from BB2 is supplied to the same bus through a voltage source current controlled (VSCC) inverter and therefore acts as a local grid by providing the needed voltage and frequency of the power plant. This means that BB2 is always connected to the bus. As a local grid, the battery through the inverter, determines and sets the voltage and frequency of operation of the hybrid energy system. Any change in real power of the system will depend on the frequency, whereas changes in reactive power will be mainly dependent on voltage. BB1 may or may not be connected to the bus depending on certain conditions which include: load demand, availability of power from the sun, and the state of charge (SOC) of the two batteries.

For effective operation of the paralleled BB1 and BB2 inverters, the inverters need to be isolated from each other by use of the transformer TX1. The isolation transformer will among other roles prevent circulation of potential zero-sequence current in the converters and avoid bridging between the parallel inverter switches.

For a more stable operation of the hybrid system, a static var compensator (SVC) for continuous reactive power output ability, high efficiency and low harmonic distortion in the output current [9] is installed which together with the battery unit fulfils the variable reactive power requirement of the induction generator and of the load.

Before reaching the intended load points, voltages from the various functional units will experience some drops at the auxiliary components and intermediate buses. Transformer TX2 is positioned to upgrade the voltage before supplying the loads.

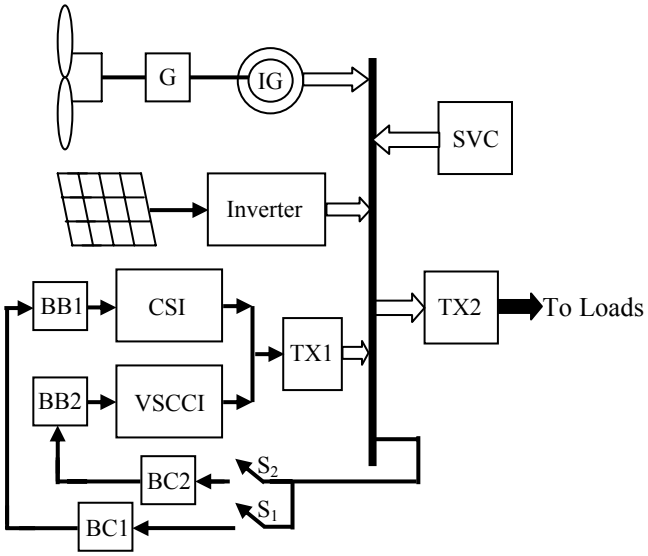

Fig. 2: The system structure for the proposed hybrid power plant.

3. System operation

The operational modes of the hybrid system may be divided into three principal modes: normal mode, complementary mode, and back-up mode. In the normal mode of operation, the load is powered by a combination of the PV power unit and the wind turbine power unit. In this mode and in other modes, battery bank BB2 acts both as a power source and a power sink as it constantly supplies power to the bus through the VSCCI and is charged through BC2. In the complementary mode, BB1 is switched into the system to complement the hybrid power from PV and wind units. This however will depend on the SOC of BB1; else an alternative power source like diesel generator (though outside the scope of this paper) may be resorted to. In the back-up mode, BB1 is switched into the system to share the load with BB2. Most times, battery banks are typically sized to supply the electrical load for up to three days, to compliment for hours/days during which neither solar nor wind power is produced. Hence, hybrid power system ensures that in the event of limited power from any of the units at a particular time/day like solar on cloudy days or no wind days, for any reason, there will be a back up means of providing the plant power.

This paper focuses on the feasibility of wind-solar hybrid power system in Nsukka. To this end, the average wind speed and solar radiation over some periods are recorded and tied to power so as to ascertain the feasibility of the wind-solar hybrid power plant in the region. The scope of this paper is therefore limited to the models describing the power generating capacity of the hybrid components.

4. Hybrid Power System Components Modeling

The two principal components in the wind-solar hybrid power system are the wind power unit and the solar power unit. Other components e.g. the battery bank – inverter and the static var compensator sub units and the detailed interactions between the principal components and the other components are not covered in this work.

4.1 Wind Power Unit

The mechanical power extracted from the wind [10] is obtained as:

$$P_{mec} = 0.5\rho\pi R^2 V_w^3 C_p(\lambda) \quad (1)$$

where P_{mec} is the power extracted from the airflow [W], ρ is the air density (about 1.225 at sea level or 1.168 at standard ambient temperature & pressure) [kg/m^3], R is the radius of the turbine blade [m], V_w is the wind speed upstream the rotor [m/s], C_p is the turbine power coefficient which represents the power conversion efficiency of a wind turbine, and λ is the tip speed ratio given by:

$$\lambda = \frac{\omega_r R}{V_w} \quad (2)$$

with ω_r the rotor angular speed [rad/s]. For every wind speed, there exists a rotor speed ω_r, at which maximum power can be extracted from a given turbine and this power is dependent upon the turbine's power coefficient $C_p(\theta,\lambda)$. This maximum power corresponds to maximum power coefficient $C_{p,max}$ and at this $C_{p,max}$ there exists a corresponding optimum tip-speed ratio λ_{opt}. Thus, for a variable speed wind turbine (i.e. variable ω_r), the optimum tip-speed ratio λ_{opt}, is maintained constant by varying ω_r in relation to the change in wind speed V_w. By this process, a variable speed wind turbine follows the $C_{p,max}$ to capture the maximum power up to the rated speed by varying the rotor speed to keep the system at the optimum tip-speed ratio λ_{opt}. For variable speed wind turbines, the following generic equation [10] may be used to approximate the power coefficient:

$$C_p(\theta,\lambda) = 0.5176\left(\frac{116}{\lambda_i} - 0.4\theta - 5\right)e^{\frac{-21}{\lambda_i}} + 0.0068\lambda \quad (3)$$

with

$$\lambda_i = \frac{1}{\frac{1}{\lambda + 0.08\theta} - \frac{0.035}{\theta^3 + 1}} \quad (4)$$

where θ is the pitch angle. The electrical output power of the induction generator may be obtained as:

$$P_{el} = \eta_{gen} P_{mec} \quad (5)$$

where η_{gen} is the generator efficiency. In eqn. (1) and hence eqn. (5) the only variable factor is the wind speed. Thus, while different values of turbine rotor speed will be established for each speed, the λ and hence C_p are maintained constant for the wind speed variations. In this research, an appreciable value of R will be chosen in order to an extent cushion the effect of the small wind resource in this region.

4.2 PV Power Unit

A photovoltaic array (PV system) is an interconnection of modules which in turn is made up of many PV cells in series or parallel. The power produced by a single module is seldom enough for commercial use, so modules are connected to form an array to supply the load. The connection of the modules in an array is same as that of cells in a module [11]. Modules can also be connected in series to get an increased voltage or in parallel to get an increased current. PV arrays are built up with combined series/parallel combinations of PV solar cells, which are usually represented by a simplified equivalent circuit model such as the one given in Fig. 3 [11], [12], [13], and [14].

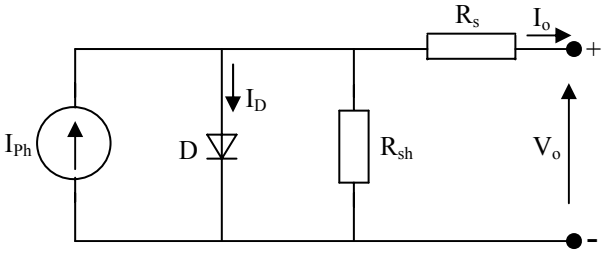

Fig. 3: Simplified Equivalent Electric circuit of a PV cell.

The power generation simulation model for the PV system is composed of three parts: PV array power model, solar radiation on PV module surface and PV module temperature model [8].

4.2.1. PV Array Power Model:

Models relating the current and voltage of a PV cell and hence PV array abound in literature [11, 15, 16]. It is clear that for the maximum power production of the PV generator, the models describing the PV module's maximum power output behaviours become more practicable. This work focuses on the PV array power model that relates the PV array power with the solar radiation and PV module temperature. The resulting relationship is obtained as [12]:

$$P_{module} = \frac{\dfrac{V_{oc}}{n_{MPP}KT/q} - \ln\left(\dfrac{V_{oc}}{n_{MPP}KT/q} + 0.72\right)}{1 + \dfrac{V_{oc}}{n_{MPP}KT/q}} \bullet \left(1 - \frac{R_s}{V_{oc}/I_{sc}}\right) \bullet I_{sco}\left(\frac{G}{G_0}\right)^{\alpha} \bullet \frac{V_{oco}}{1 + \beta \ln\dfrac{G_0}{G}} \bullet \left(\frac{T_0}{T}\right)^{\gamma} \quad (6)$$

where n_{MPP} is the ideality factor at the maximum power point ($1 < n_{MPP} < 2$). It is assumed that the PV module working states revolve around the maximum power point. K is the Boltzmann constant (1.38×10^{-23} J/K); T is the PV module temperature, K; q is the magnitude of the electron charge (1.6×10^{-19} C); R_s is the series resistance, Ω; α is the factor responsible for all the nonlinear effects that the photocurrent depends on; β is a PV module technology specific-related dimensionless coefficient; and γ is the factor considering all the nonlinear temperature–voltage effects. G_0 and G_1 represent two different solar irradiance intensities, while T_0 and T_1 represent two PV module temperatures.

The five parameters (α, β, γ, R_s and n_{MPP}) which appear in equation (6) are introduced to take into account all the nonlinear effects of the environmental factors on PV module performance. In order to calculate the five parameters, the parameters of the PV module supplied by the manufacturers e.g. the short-circuit current I_{sc}, open-circuit voltage V_{oc}, maximum power point current I_{MPP} and voltage V_{MPP} of the PV module under two different solar irradiance intensities (G_0, G_1) and two PV module temperatures (T_0, T_1) are used. Table 1 shows the estimated parameters [12]. These parameters obtained from the PV module specifications shown in Table 2 are used in conjunction with the module parameters to estimate the PV power output.

Table 1: Parameter estimation results for the PV module performance

α	β	Γ	R_s	n_{MPP}
1.21	0.058	1.15	1.17	0.012

Table 2: Specifications of the PV module

V_{oc}(V)	I_{sc}(A)	V_{max}(V)	I_{max}(A)	P_{max}(W)
21	6.5	17	5.73	100

PV modules represent the fundamental power conversion unit of a PV system. For a matrix of Ns x Np PV modules, the maximum power output of the PV system can be calculated by:

$$P_{PV} = N_p \cdot N_s \cdot P_{module} \cdot \eta_{MPPT} \cdot \eta_{oth} \tag{7}$$

where N_p is the number of modules in parallel, N_s is the number of modules in series, η_{MPPT} is efficiency of the maximum power point tracking. Although η_{MPPT} varies according to different working conditions, a constant value of 95% is assumed to simplify the calculations. η_{oth} is the factor representing the other losses such as the loss caused by cable resistance, accumulative dust, etc. Thus, once the solar radiation on the module surface and the PV module temperature are known, the power output of the PV system can be predicted.

4.2.2. Solar Radiation on PV Module Surface:

The power incident on a PV module depends not only on the power contained in the sunlight, but also on the angle between the module and the sun. The amount of solar radiation incident on a tilted module surface is the component of the incident solar radiation which is perpendicular to the module surface. Fig. 4 shows how to calculate the radiation incident on a titled surface (G_{module}) given either the solar radiation measured on horizontal surface (G_{horiz}) or the solar radiation measured perpendicular to the sun ($G_{incident}$) [17].

Radiation incident on a titled module surface from Fig. 4 can be expressed as:

$$G_{mod} = G_{inc} \sin(\alpha + \theta) \tag{8}$$

where α is the elevation angle, and θ is the tilt angle of the module measured from the horizontal. The elevation angle may be obtained as:

$$\alpha = 90 - \phi + \delta \tag{9}$$

where is the latitude; and δ is the declination angle given as:

$$\delta = 23.45^{o} \sin\left[\frac{360}{365}(284 + d)\right] \tag{10}$$

where d is the day of the year. The tilt angle has a major impact on the solar radiation incident on a surface. For a fixed tilt angle, the maximum power over the course of a year is obtained when the tilt angle is equal to the latitude of the location [17].

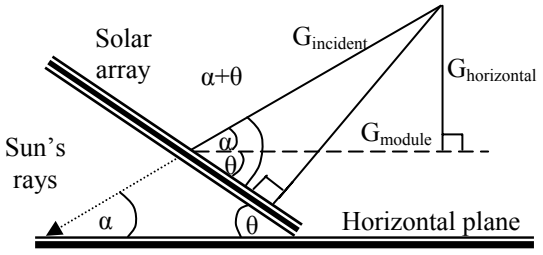

Fig. 4: How to calculate the radiation incident on a titled surface.

In modeling the PV power unit, the effect of the PV inverter should be taken into account as component of the PV power unit. In practical applications, it is usual to observe that power generated from the PV array at any given period is higher than the power delivered to the bus through the inverters. Between 7 per cent and 19 per cent of power generated from the PV array are lost in the inverters. Thus, in addition to connection losses and other losses such as the ones caused by accumulative dust on the array, a factor to account for the losses in the inverter must be included. Inverter switching losses and losses due to non-ideal components account for the increase in average temperatures in the PV inverters. The average temperatures in the PV inverters have been observed to be almost twice the temperatures in PV array, even as the modules are in direct contact with sunlight [18].

4.2.3. PV Module Temperature Model:

Based on energy balance, the PV cell operating temperature can be expressed as follows [13], [19]:

$$T_c(t) = 273.15 + 3.12 + 0.25G + 0.899T_a - 1.3V_{\omega} \tag{11}$$

where G is the PV module solar insolation, T_a is the ambient temperature (^{o}C), and V_w is the wind speed.

Most local observatories provide only solar irradiation data on a horizontal plane. Thus, an estimate of the solar irradiation incident on any sloping surfaces as analyzed in section 4.2.2 shall be applied.

5. Application to a case study

The feasibility of a stand alone wind-solar hybrid power system in a low wind region is investigated using the real data obtained from the Centre for Basic Space Science, University of Nigeria, Nsukka. The data of the First March and First July 2010 are used. They consist of the hourly wind speed, solar insolation, and ambient temperature. The use

of data obtained at two extreme weather conditions (hot season and rainy season) is to study the viability of the hybrid system in meeting an all year round demand of a sample load. Figs. 5 and 6 show the hourly wind speed variations for March and July respectively. Figs. 7 and 8 show the hourly solar insolations for March and July respectively while Fig. 9 displays the hourly temperature variation for the two months.

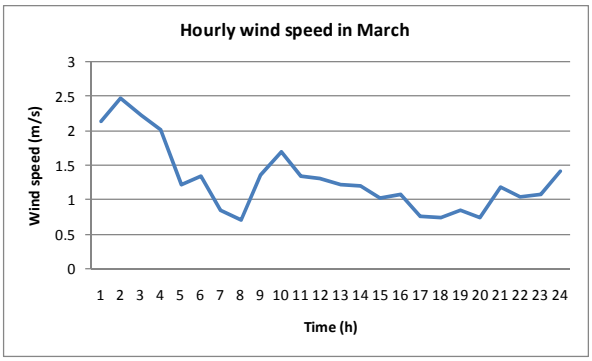

Fig. 5: Hourly wind speed variation in March.

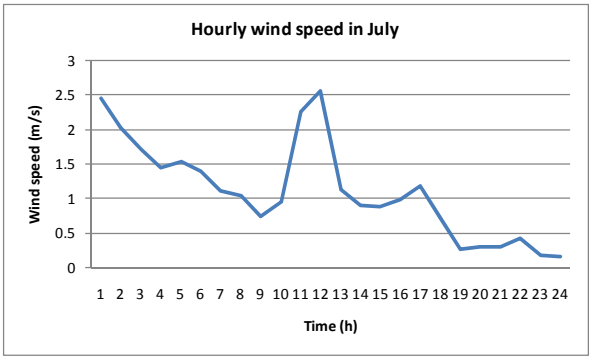

Fig. 6: Hourly wind speed variation in July.

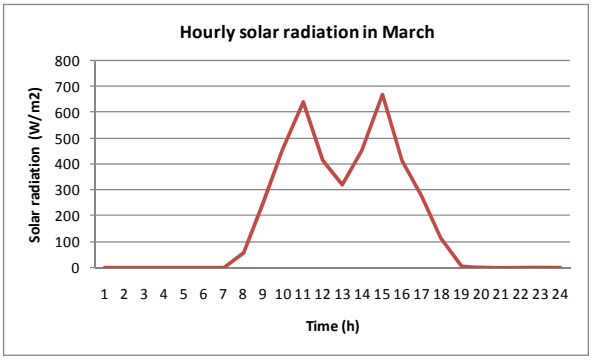

Fig. 7: Hourly solar insolation in March.

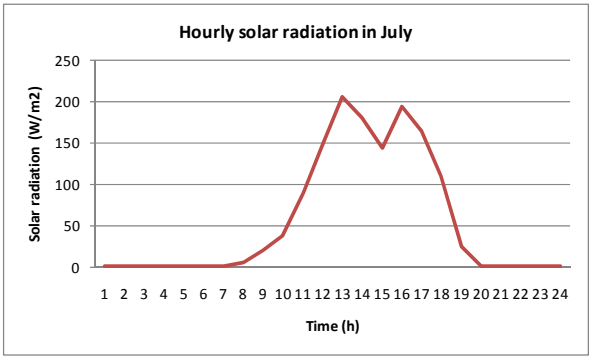

Fig. 8: Hourly solar insolation in July.

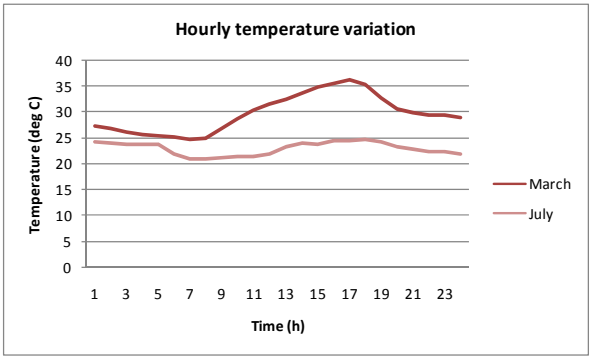

Fig. 9: Hourly temperature variations in March and July.

6. Data applications

The acquired data as represented in Figs. 5 to 9 are processed with a view to generating electric power to meet a sample load. The load profile is patterned after a load demand of an average 3-bedroom flat apartment.

6.1. Wind power

It is usual to specify the operating wind speed range, the cut-in wind speed and the rated wind speed. In this feasibility analysis, however, all the extractable wind power within the resource region are shown. A 25m turbine rotor radius is used in the variable speed wind turbine. In generating the mechanical wind power using eqn. (1) and hence the electrical power using eqn. (5), only the hourly wind speed is utilized from the three data comprising the wind speed, solar insolation, and air temperature. From each wind speed data, the maximum power coefficient $C_{p,max}$, is derived with the aid of the rotor radius. At the $C_{p,max}$, the maximum power at any given wind speed is extracted.

6.2. Solar power

In order to generate the PV array solar power using eqns (6) and (7), the three recorded data are involved. They are further processed through eqns. (8) to (11) in order to generate the solar insolation G, and the temperature T, for the PV module power in eqn. (6). In determining the amount of solar radiation incident on a tilted module surface, the chosen tilt

angle of the PV module is used in conjunction with the angle of elevation which in turn depends on the day of the year being considered. The solar radiation incident on a tilted module surface, the ambient temperature T_a, and the wind speed data are used to obtain the PV cell operating temperature. Table 3 shows all the data needed for the generating of the PV array power.

Table 3: Data for the generating of PV array power.

N_p	N_s	η_{oth}	$T_o(^oK)$	$G_o(W/m^2)$	$\theta(^o)$	$\prod(^o)$
2	6	0.89	295.15	96	30	7

7. Results and discussion of results

Fig. 10 shows the hourly power produced by the wind turbine, as well as the hourly power produced by the PV array. The high power yield of the PV array over the wind turbine is a true reflection of the amount of solar radiation over the wind speed in the region. Fig. 11 shows the power generated from the hybrid components and the power demand by the load in 1st March 2010. Within major part of the day, the hybrid system appear capable of supplying the load, while at some part of the day the load demand exceeds the power from the hybrid components. At these points especially during the sunless hours, a combination of the wind power and the power from the battery bank can effectively supply the load with less stress on the battery bank power. The excess power from the PV array during the sun hours and part of the wind power can be channeled to the charging of the battery bank.

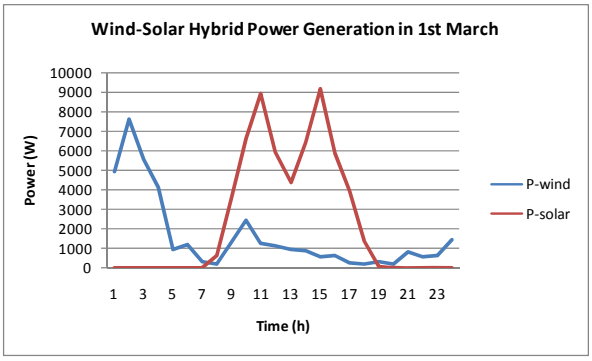

Fig. 10: Hourly power produced by the wind turbine and the PV array in 1st March.

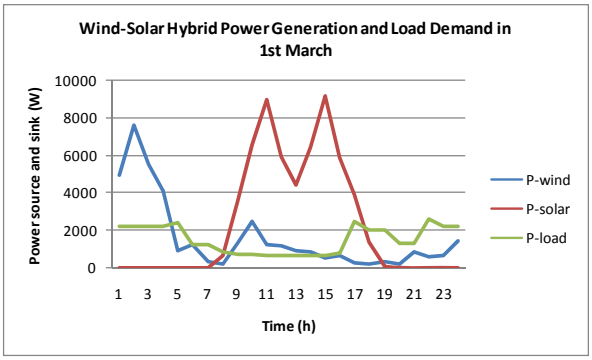

Fig. 11: Hourly power produced by the hybrid plant and the load demand in 1st March.

Fig. 12 is similar to Fig. 10 but with a reduced PV array power which explains the difference in solar radiation between the two periods of the year. Fig. 13 shows a different load pattern from that of Fig. 11 especially during the night period when less power is demanded. Like in Fig. 11, battery bank power can effectively supply the load at periods of hybrid power deficiency. Power from the hybrid plant at the periods of excess are used to charge the battery bank. Fig. 14 shows the solar PV array power in 1st March and in 1st July. The peak and average solar power generated in 1st March are both above 4 times the amount generated in 1st July. This demonstrates the fact that large amount of solar radiation falls in March than in July. Fig. 15 displays the wind turbine power in 1st march and in 1st July.

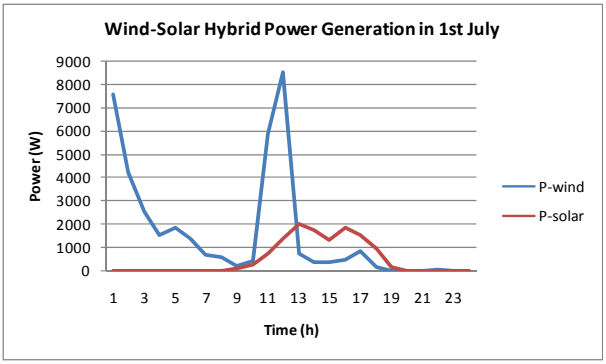

Fig. 12: Hourly power produced by the wind turbine and the PV array in 1st July.

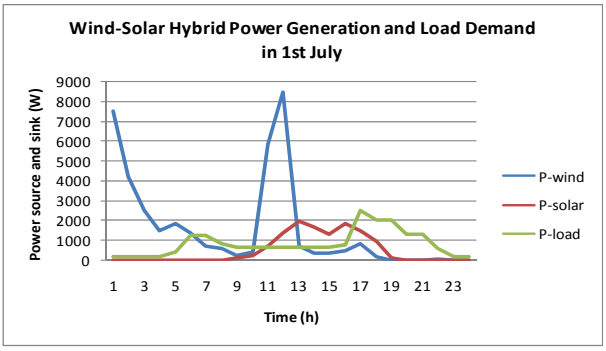

Fig. 13: Hourly power produced by the hybrid plant and the load demand in 1st July.

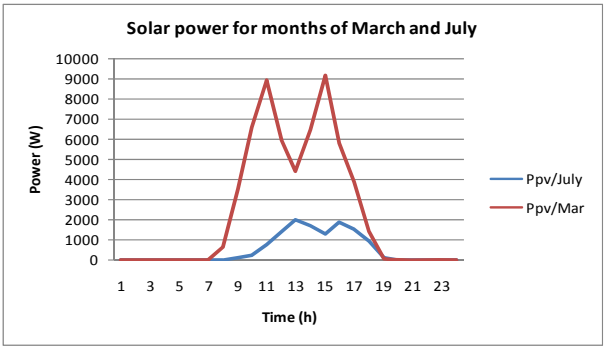

Fig. 14: Comparism of the hourly power produced by the solar PV array in 1st march and 1st July.

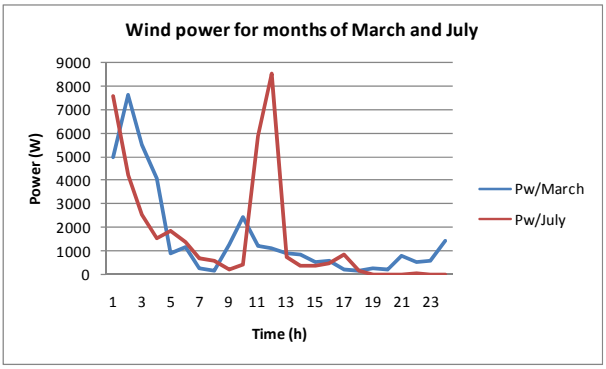

Fig. 15: Comparism of the hourly power produced by the wind turbine in 1st march and 1st July.

8. Conclusion

A feasibility study of wind-solar hybrid power system in South Eastern Nigeria has been presented. Hourly recorded data comprising the wind speed, the solar insolation, and air temperature at the Centre for Basic Space Science University of Nigeria, Nsukka has been applied to meet the power demand of a typical 3-bedroom flat apartment. It is observed that the hybrid plant is able to satisfy the daily average load demand of about 1.5 kW during hot season and less than 1.0 kW during rainy season. Excess power from the hybrid can be used to charge the battery bank which in turn supplies the load in the event of hybrid power deficiency.

References

[1] Hybrid Power Systems – Issues & Answers, Available Online *03-08-2011*: http://photovoltaics.sandia.gov/docs/Hybook.html

[2] Travelmath, Available Online *03-08-2011*: www.travelmath.com/country/Nigeria

[3] Nwosu CA, Agu MU. "Power and Energy Balance in Wind-Solar Hybrid Power System," *Pacific Journal of Science and Technology*, vol 10, 2009, pp. 110-116.

[4] Nwosu CA. "Renewable Resources in Dispersed Generation: Solution to Nigeria's Electric Energy Crises," *Proc. on ESPTAE National Conference, University of Nigeria, Nsukka*, 25th – 27th June, 2008, pp. 207 – 216.

[5] Halasa G. "Wind-Solar Hybrid Electrical Power Generation in Jordan," *Jordan Journal of Mechanical and Industrial Engineering*, vol. 4, Jan. 2010 pp. 205 – 209.

[6] Yang H, Lu L, Zhou W. "A novel optimization sizing model for hybrid solar-wind power generation system," *ScienceDirect – Solar Energy*, vol. 81, Jan. 2007, pp. 76 – 84.

[7] Ogwo U. "The Place of Wind Energy in Checking the Menace of Power Outages in Nigeria," *2nd International Renewable Energy Conference (IREC) Lagos, Nigeria*, Oct. 2007. Available Online *07-08-2011*: http://www.solartimeelectric.net/page6.html

[8] Ajao KR, Oladosu OA, Popoola OT. "Using Homer Power Optimization Software for Cost Benefit Analysis of Hybrid-Solar Power Generation Relative to Utility Cost in Nigeria," *International Journal of Research and Reviews in Applied Sciences*, vol. 7, 2011, pp. 96 – 102.

[9] Yao G, Tao L, Zhou L, Chen C. "State-feedback Control of a Current Source Inverter-based STATCOM," Available Online *10-08-2011*: http://www.docstoc.com/docs/28657571/

[10] Slootweg JG. *Wind Power Modeling and Impact on Power System Dynamics*, PhD Thesis, Delft University of Technology, (TU-Delft), the Netherlands, 2003.

[11] Narkhede S, Rajpritam. *Modeling of Photovoltaic Array,* BTech Thesis, Department of Electrical Engineering National Institute of Technology Rourkela-769008, Orissa.

[12 Yang H, Lu L, Zhou W, Fang Z. "Optimal sizing method for stand-alone hybrid solar-wind system with LPSP technology by using genetic algorithm," *ScienceDirect – Solar Energy*, vol. 82, 2008, pp. 354 –367.

[13] Kamath H, Aithal RRS, Singh PK, Danak AR. "Modeling of Photovoltaic Array and Maximum Power Point Tracker Using ANN," Available Online *10-08-2011*: http://www.esrgroups.org/journal/jes/papers/

[14] Altas IH, Sharaf AM. "A Photovoltaic Array Simulation Model for Matlab-Simulink GUI Environment," Available Online: www.mendeley.com/.../photovoltaic-array-simulation
[15] Joyce A, Rodrigues C, Manso R. "Modeling a PV system," *ScienceDirect – Renewable Energy*, vol. 22, iss. 1 – 3, Jan – March 2007, pp. 275 – 280.
[16] Kamath HR, Aithal RS, Singh PK, Kumar A, Danak AR. "Modeling of Voltaic Array and Maximum Power Point Tracker Using ANN," Available Online *02-09-2011*: www.esrgroups.org/journal/jes/papers/4_3_4
[17] Available Online *10-09-2011*: http://pvcdrom.pveducation.org/SUNLIGHT/MODTILT.HTM
[18] Asomba GC, Nwosu CA. "Analysis and Validation of Power Conversion Efficiency in PV System," *Pacific Journal of Science and Technology*, vol. 9, pp. 337-343, 2008.
[19] Belfkira R, Reghem P, Raharijaona J, Barakat G, Nichita C. "Non Linear Optimization Based Design Methodology of Wind/PV Hybrid Stand Alone System," Available Online *11-09-2011*: http://cmrt.centrale-marseille.fr/cpi/ever09/documents/.../EVER09-paper-152